ISBN: 978-3-95450-221-9 ISSN: 2226-0358 doi:10.18429/JACoW-ICALEPCS2021-TUPV001

Content from this work may be used under the terms of the CC BY 3.0 licence (© 2022). Any distribution of this work must maintain attribution to the author(s), title of the work, publisher, and DOI

THE MIRROR SYSTEMS BENCHES KINEMATICS DEVELOPMENT FOR SIRIUS/LNLS*

G. N. Kontogiorgos†, A. Y. Horita, L. M. Santos, M. A. L. Moraes, L. F. Segalla,
Brazilian Synchrotron Light Laboratory (LNLS), Campinas, Brazil

Abstract

At Sirius, many of the optical elements such as mirror systems, monochromators, sample holders and detectors are attached to the ground with high stiffnesses to reduce disturbances at the beam during experiments [1]. Granite benches were developed [2] to couple the optical device to the floor and allow automatic movements, via commanded setpoints on EPICS [3] that runs an embedded kinematics, during base installation, alignment, commissioning and operation of the beamline. They are composed by stages and each application has its own geometry, a set number of Degrees-of-Freedom (DoF) and motors, all controlled by Omron Delta Tau Power Brick LV. In particular, the mirror system was the precursor motion control system for other benches [4 - 6]. Since the mechanical design aims on stiffness, the axes of mirror are not controlled directly, the actuators are along the granite bench. A geometric model was created to simplify the mirror operation, which turn the actuators motion transparent to the user and allow him to directly control the mirror axes.

INTRODUCTION

The latest Sirius mirror bench mechanical design version will be installed in Mogno and Ipê beamlines. They are composed by three stacked granites pieces (Fig. 1), the first one is supported by three levellers on the floor, the second is above the first and it has a ramp to form a wedge with the third granite.

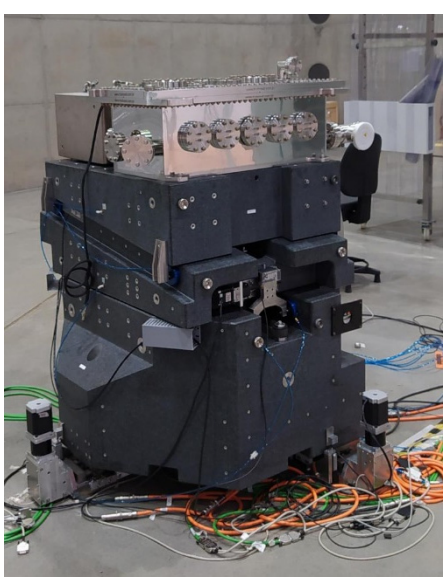

Figure 1: Granite assembly before installation and commissioning.

The mirror positioning depends on the relative motion between those components. Air-bearings were disposed both to guide and lift the granites between interfaces. The pressure, flow and activation of the air-bearings are commanded by a pneumatic panel.

KINEMATICS

Kinematic Model

As mentioned, the hole granite stack is supported by three levellers (The leveller is the component A of Fig. 2). They do not have feedback sensor, the position is measured by three Heidenhain gauges (Component B of Fig. 2) which touch the granites, so the measurement is done at the bench itself, not on the actuator. Although the controller can read the real position of the granite, this mechanical design allows the granite to slide over gauge and the leveller. This result presents incoherence between real position and the controller readback position. Furthermore, the geometry is much more complicated when considering friction and sliding on mechanics. To contour those problems, approximations were done on the geometry (As will be shown now) and an iterative actuation was developed (As will be shown later).

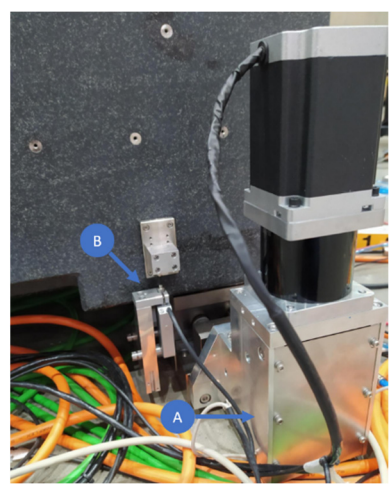

Figure 2: Leveller actuator (A) and feedback encoder (B).

The levellers could be interpreted as a parallel robot called tripod. The tripod was modelled using two reference frames [7], one rigidly coupled to the top platform (S_1), which is the moving one, and the other frame is at rest on the laboratory (S_0). Three vectors $\vec{r}_i(S_1)$ $i = 1, 2, 3$, connect the S_1 origin to the three vertical Heidenhain sensors points that touch the platform. This is the first approximation of this model. Figure 3 illustrates both reference

ISBN: 978-3-95450-221-9 ISSN: 2226-0358 doi:10.18429/JACoW-ICALEPCS2021-TUPV001

frames, the vectors for each sensor and their projection on the sensors axes represented at laboratory reference frame.

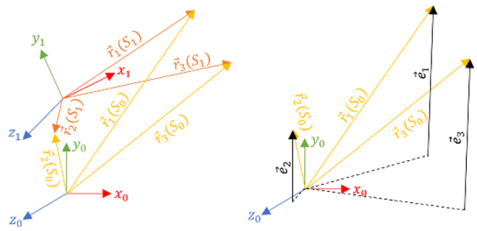

Figure 3: Referential transformation for tripod, part of mirror system kinematics.

The relationship between both reference frames is described by two rotations (R_x, R_z) and one translation about $\hat{y}_0$ axis (q_3), which are the allowed DoF for a tripod robot. Using the homogeneous transformation matrices T, it was possible to find the representation of the vectors rigidly coupled to S_1 on S_0 frame, the $\vec{r}_i(S_0)$ $i = 1, 2, 3$, which is the frame where the encoders are.

$$\begin{cases} \vec{r}_1(S_0) = T(R_x, R_z, q_3)\vec{r}_1(S_1) \\ \vec{r}_2(S_0) = T(R_x, R_z, q_3)\vec{r}_2(S_1) \\ \vec{r}_3(S_0) = T(R_x, R_z, q_3)\vec{r}_3(S_1) \end{cases} \tag{1}$$

The sensors movement are limited into $\hat{y}_0$ direction and the projection of the vectors represented on S_0 frame system onto $\hat{y}_0$ direction gives us the sensors positions $e_i, i = 1, 2, 3$.

$$\begin{cases} e_1(R_x, R_z, q_3) = |\vec{e}_1| = \hat{y}_0 \cdot \vec{r}_1(S_0) \\ e_2(R_x, R_z, q_3) = |\vec{e}_2| = \hat{y}_0 \cdot \vec{r}_2(S_0) \\ e_3(R_x, R_z, q_3) = |\vec{e}_3| = \hat{y}_0 \cdot \vec{r}_3(S_0) \end{cases} \tag{2}$$

Those relationships are usually called the inverse kinematics because they express the "actuator" position in function of the desired DoF's (on robotics these desired positions usually are the tool positions).

To couple the tripod to the granite actuators a transformation from parallel robot into serial robot was performed. The forward kinematics of the tripod is now necessary since each DoF represented in terms of the encoders could be transformed into an actuator of a serial robot. This set of equations are non-linear and finding the forward kinematics analytically is not possible. There are two ways of solving it: approximation by Taylor expansion and numerical methods. Since the angles are small and it would reduce the complexity of solution, the small angle approximation was chosen and the inversion of the linear system became possible.

The first air interface, shown on Fig. 4 item D, between the first and second granite has three actuators: one on the $\hat{x}_0$ direction (item C) and the others on the $\hat{z}_0$ direction (item B, the other cannot be seen from a single view because it is on the other side of the granite).

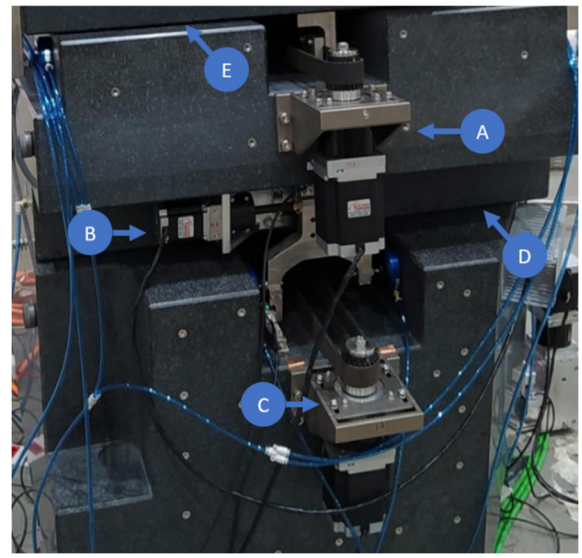

Figure 4: Granites' disposition of actuators and interfaces of granite bench.

Both $\hat{z}_0$ direction actuators can perform rotation (R_y) towards an axis parallel to $\hat{y}_0$ and translations (q_3) on an axis that is parallel to $\hat{z}_0$ if the motion is done in a coordinated way. The problem of transforming actuators into serial joints arises again since the z actuators forms a parallel robot. Some geometrical analysis led us to the following expressions:

$$\begin{cases} q_3 = \frac{z_{upper}d_{upper} + z_{lower}d_{lower}}{d_{upper} + d_{lower}} \\ R_y = \arctan \frac{\theta_{wedge}}{|\theta_{wedge}|} \frac{z_{lower} - z_{upper}}{d_{upper} + d_{lower}} \end{cases}. \tag{3}$$

Where z_i is the actuator position, d_i is the distance from the desired R_y pivot axis parallel to $\hat{y}_0$ axis to the $\hat{z}_0$ actuator and θ_{wedge} is the wedge angle (both $i = upper, lower$). This last parameter is only required to set the equations orientation, since the beamlines designers set the bench orientation according to their needs.

The last actuator (on granite bench because the internal mechanism has the piezo actuator) is the Fig. 4 item A, the wedge actuator, control the movement to lift the third granite through the ramp. Some caution must be taken here about the movement of the wedge, since it is used to lift the mirror parallel to $\hat{y}_0$ axis in the case that all rotations are zero. Although the pure movement may present undesired parasite motion, the hole inverse kinematics working together (this will be discussed further).

With all actuators properly modelled, a kinematics scheme could be synthetized in a serial robot model, Fig. 5.

Content from this work may be used under the terms of the CC BY 3.0 licence (© 2022). Any distribution of this work must maintain attribution to the author(s), title of the work, publisher, and DOI

ISBN: 978-3-95450-221-9 ISSN: 2226-0358 doi:10.18429/JACoW-ICALEPCS2021-TUPV001

Content from this work may be used under the terms of the CC BY 3.0 licence (© 2022). Any distribution of this work must maintain attribution to the author(s), title of the work, publisher, and DOI

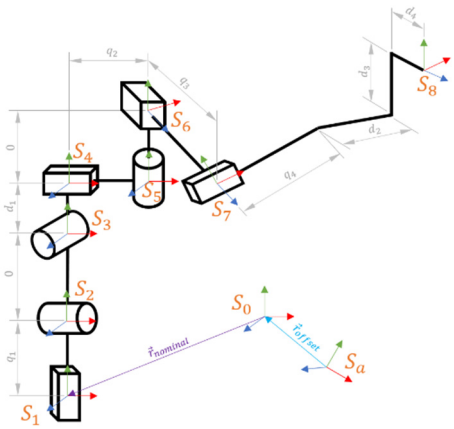

Figure 5: Mirror system kinematic scheme.

The scheme $\vec{r}_{nominal}$ is the fixed machine offset from the first joint to the control point S_8, usually set on the center of the mirror. This point is interesting because you are always commanding the positions to the mirror near the specified beamline mirror center. The $\vec{r}_{offset}$ is the user offset and was created to correct alignment positions or to set new positions to the mirror center as user want. The q_i , $i = 1 \ldots 4$ are the variable translations performed by the actuators and the d_i , $i = 1 \ldots 4$ are the fixed offsets between the joints. The levelers transformations results onto joints on S_1, S_2, S_3, the $\hat{x}_0$ direction actuator (Item C, Fig. 4) is the S_4 actuator, the composed movement in Eq. (3) with B actuators are performed by S_5 and S_6 joints and the last one, the S_7 joint is rotated by θ_{wedge} angle to model the wedge. The forward kinematics is totally modelled with this scheme and the rotations R_x, R_y, R_z and translations U_x, U_y, U_z could be found in function of the encoders.

Kinematics by Steps

There is no mechanism on levellers-granite interface that locks the parasite motion and the entire system can drift along undesired axes during some commanded movement. A hypothesis from mechanical design group is that a segmented movement instead of usual closed loop control would be a better approach to avoid this problem.

The proposal is setting the actuators in open loop while three encoders guarantee that each motor reach their specific position during the process.

The user would be able to define a threshold, which controls how close to the exact final position the levellers should get. At each iteration of the algorithm the position of the levellers is compared to the desired position, by reading the virtual motors. While their position is not inside the threshold band a new step is calculated based on the distance from the final position, them the motors are commanded to move several counts equivalent to the step. Once they reach this new position, the reference is compared again and the process continues. Figure 6 shows the state machine representation of the algorithm.

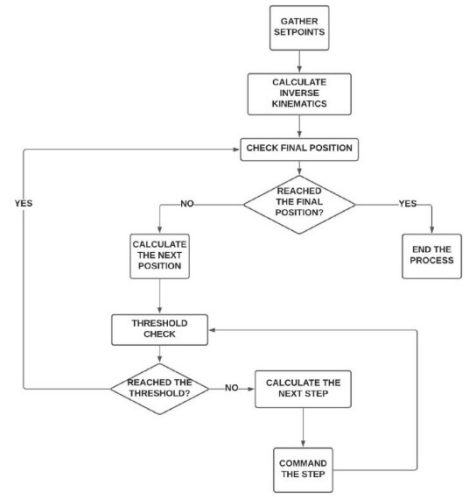

Figure 6: State machine representation of the kinematics by steps algorithm.

Numeric Solution for Inverse

The core of mirror kinematics is the inverse kinematics calculation since it gives the setpoints for actuators control loop. The user inputs for inverse kinematics are the DoF $\vec{u} = (R_x, R_y, R_z, U_x, U_y, U_z)$ of the granite bench at the control point S_8, related to S_a, the laboratory reference frame. The forward kinematics is a non-linear set of equations and finding its solution analytically is impossible. Then, the Newton method [8] was chosen for finding iteratively the encoders readings corresponding to some user input. The forward kinematics can be written as:

$$\vec{u} = \vec{f}(\vec{e}). \tag{4}$$

Where $\vec{e}$ is the actuators or encoders positions vector and note that $\vec{u}$ is the output vector on forward kinematics but it is the input on inverse as we are going to see. Let us define an error function $\vec{G}$, which is going to be minimized

$$\vec{G}(\vec{e}, \vec{u}) \triangleq \vec{f}(\vec{e}) - \vec{u}. \tag{5}$$

The method iteration can be defined as

$$\vec{e}_{k+1} = \vec{e}_k + \mathcal{J}^{-1}(\vec{e}_k)\vec{G}(\vec{e}_k, \vec{u}). \tag{6}$$

Where $\mathcal{J}$ is the Jacobian matrix of $\vec{f}$ and k is the iterator index. The iteration loop stops by the norm of $\vec{e}_{k+1}$ condition, which must be less than one count.

TESTS AND VALIDATIONS

The mirror kinematics validation was done by an external set of instruments. Six Heidenhain gauges were positioned in such a way to get the last granite position (Fig. 7).

ISBN: 978-3-95450-221-9 ISSN: 2226-0358 doi:10.18429/JACoW-ICALEPCS2021-TUPV001

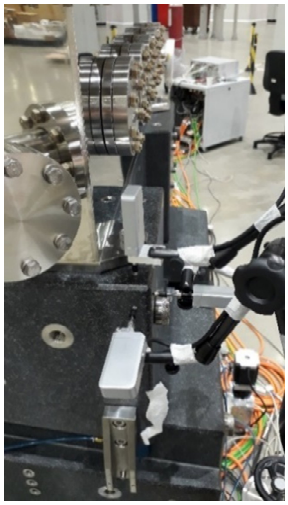

Figure 7: Setup for the kinematic validation.

Each granite surface which is touched by the gauges is modelled as a plane generated by three known points from the metrology data. Those points are fixed on the granite reference frame (e.g. this frame could be chosen) and a coordinate transformation with respect to $\vec{u}^{meas} = (R_x^{meas}, R_y^{meas}, R_z^{meas}, U_x^{meas}, U_y^{meas}, U_z^{meas})$ allows the representation of those points on the laboratory reference frame. The Heidenhain gauges measurement are represented by one of three coordinates of the plane equation while the other coordinates are the gauges' location on the plane, which has been obtained from metrology measurements.

The model described above gives the gauges positions in function of the coordinates $\vec{u}^{meas}$. The validation of kinematics can be done by the Newton-Raphson method, since $\vec{u}^{meas}$can be found in function of gauges data. Each DoF was subject to a programmed movement on PowerPMAC using the developed kinematics and each gauge position was gathered with another PowerPMAC controller.

Some data were corrupted during the gather and not all analysis could be done in this paper, which is going to be done in future works. The useful data could be compiled in Table 1 and Fig. 8 illustrates the control data and post processed data from the measurement devices.

Table 1: Formatting of References

Parameter	Rx	Rz
Accuracy	3.44e-1	6.16e-1
Rx drift	3.44e-1	2.04e1
Ry drift	3.57e-2	5.71e-3
Rz drift	2.87e-1	1.79e1
Tx drift	2.94e3	1.01e1
Ty drift	1.95e1	1.70e2
Tz drift	8.64e1	1.52e2

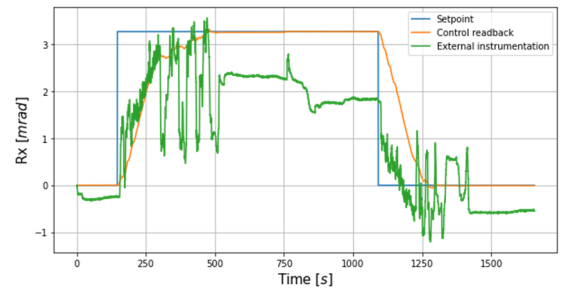

Figure 8: Measurement of a rotation towards x-axis done by mirror controller system and by validation method.

The accuracy is the difference of setpoint and the mean value of the measured data at the end of motion. The drifts are the difference from the position immediately before and the position after that this step motion is undone, which should be ideally zero.

CONCLUSION

The kinematics play an important role during beamline operation since it improves the user experience on its devices. Commissioning, alignment and operation are much easier when the user controls the mirror axes directly and no hand calculation is needed to find the positions of the actuators to perform a pure movement on the mirror.

Some tests were performed recently to characterize the motion of the system being operated by kinematics interface. A validation methodology was developed and now it can be improved and applied on the next beamline bases since some data was corrupted during tests before installation. Although there were problems, the present analysis offered several information for further project improvements.

REFERENCES

[1] C. S. N. Bueno *et al.*, "Vibration Assessment at the CARNAÚBA Beamline at Sirius/LNLS", *in Proc. MEDSI'20*, Chicago, USA, July 2021, paper MOPB08.

[2] R. R. Geraldes *et al.*, "The Design of Exactly-Constrained X-Ray Mirror Systems for Sirius", *in Proc. MEDSI'18*, Paris, June 2018, paper WEOAMA04. doi:10.18429/JACoW-MEDSI2018-WEOAMA04

[3] pmac, https://github.com/dls-controls/pmac.

[4] R. R. Geraldes *et al.*, "The New High Dynamics DCM for Sirius", *in Proc. MEDSI'16*, Barcelona, Spain, Sep. 2016, paper TUCA05. doi:10.18429/JACoW-MEDSI2016-TUCA05

[5] L. Martins dos Santos *et al.*, "The Control System of the Four-Bounce Crystal Monochromators for Sirius/LNLS Beamlines", presented at ICALEPCS'21, Shangai, China, Oct. 2021, paper TUPV003.

[6] C. S. N. Bueno *et al.*, "Position Scanning Solutions at the TARUMÃ Station at the CARNAÚBA Beamline at Sirius/LNLS", presented at ICALEPCS'21, Shangai, China, Oct. 2021, paper WEPV002.

[7] M. W. Spong and M. Vidyasagar, *Robot Dynamics and Control*. New York, NY, USA: John Wiley & Sons, Inc., 1989.

[8] M. A. Gomes Rugiero and V. L. Da Rocha Lopes, "Introdução à resolução de sistemas não lineares", in *Cálculo Numérico – Aspectos Teóricos e Computacionais*, Ed. São Paulo, SP, Brazil: Pearson Makron Books, 1997, pp. 197-200.

Content from this work may be used under the terms of the CC BY 3.0 licence (© 2022). Any distribution of this work must maintain attribution to the author(s), title of the work, publisher, and DOI